KLE Society's
KLE Technological University, Hubballi.

A Project Phase one

Report on

"Attention Guided CNN based Lung Cancer Prediction"

Submitted in partial fulfillment of the requirement for the degree of

Master of Technology

in

Computer Science and Engineering

Submitted by

Swetha Kulkarni

01FE20MCS007

Under the guidance of

Dr. Shrinivas. D.Desai

SCHOOL OF COMPUTER SCIENCE AND ENGINEERING

Hubballi – 580 031

KLE Society's

KLE Technological University, Hubballi.

2021 - 2022

SCHOOL OF COMPUTER SCIENCE AND ENGINEERING

CERTIFICATE

This is to certify that project Phase one project entitled "**Attention Guided CNN based Lung Cancer Prediction** "is a bonafied work carried out by the student **Ms.Swetha Kulkarni–01FE20MCS007**, In partial fulfillment of the completion of 3 rd semester M.Tech course during the year 2020 – 2021. The project report has been approved as it satisfies the academic requirement with respect to the project work prescribed for the above said course.

Guide	P. G. Coordinator	Head, SOCSE
Dr. Shrinivas. D.Desai	Dr.vishwanath .P Baligar	Dr.Meena.S.M

External Viva: Name of Examiners Signature with date

1.
2.

ABSTRACT

Prediction of lung cancer is important because lung cancer will destroy the normal lung and make it hard for oxygen to get into our blood. The main causes of lung cancer are smoking and consuming tobacco products, as well as exposure to second-hand smoke. The existing model will classify cancer and non-cancer. X-ray images. Some of the x-rays may not be clear or be more detailed. The research gap is that the reported literature has not considered gamma features such that the images are more detailed and clear, which can be applied in training along with images for more accuracy. The main aim of our paper is to predict lung cancer and add the gamma features. In this paper, we are using a densenet121 model for prediction of x-ray images and gamma features to get more detailed images, which will remove the noise from the x-ray images if the x-ray images are not clear or detailed. As an experimental result, we have achieved an F1 score of 83%, sensitivity of 54%, and specificity of 100% for 20 epochs over the existing projects. The gamma corrective action plays a critical role when the gamma value is greater than 0.

Keywords: Lung cancer, Gamma correction, Chest X-ray images.

ACKNOWLEDGEMENT

The satisfaction and euphoria that accompany the successful completion of any task would be incomplete without the mention of a number of individuals whose professional guidance and encouragement helped me in the successful completion of this report work.

We take this opportunity to thank Dr. Ashok Shettar, Vice-chancellor and to Dr. N H Ayachit, Registrar, KLE Technological University, Hubballi.

We also take this opportunity to thank Dr. Meena S M, Professor and Head of Department, Department of Computer Science and Engineering for having provided us academic environment which nurtured our practical skills contributing to the success of our project.

We sincerely thank our guide Dr. Shrinivas. D.Desai, Professor, Department of Computer Science and Engineering for his guidance, inspiration and wholehearted co-operation during the course of completion.

We sincerely thank our project co-ordinator Dr. v p Baligar for his support, inspiration and wholehearted co-operation during the course of completion.

Our gratitude will not be complete without thanking the Almighty God, our beloved parents, our seniors and our friends who have been a constant source of blessings and aspirations.

Swetha kulkarni - 01FE20MCS007

CONTENTS

LIST OF FIGURES

List of Tables

Chapter 1

INTRODUCTION

In this chapter, we are discussing. In this introduction, motivation, literature survey, problem statement, and objectives are presented. According to the World Health Organization [1,] approximately 8 million deaths have been reported in 2019, primarily due to chest cancer. About fifteen per cent of smokers often develop carcinoma and succumb to death not only from chest cancer but also from other smoking-related diseases like cardiopathy, stroke, or emphysema. Detection of carcinoma in early stages plays an important role in treating the patients and also taking precautionary measures. In step with the study, the survival rate, patients with non-smoking habits do have a better life (more than 5 years) as compared to smoking patients.

Chest x-rays are painless, non-invasive tests that produce detailed chest radiographs, which is the more commonly preferred diagnostic mechanism in examining patients. Basically, X-ray uses electromagnetic waves and radiation to make pictures of our bodies. The procedures involve positioning the body between the machine that produces the X-rays and a plate that makes the image digitally or with photographic film [2].

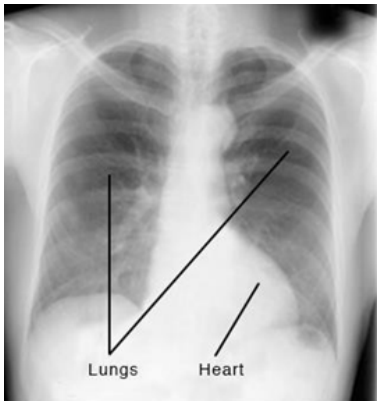

Figure 1.1: Normal chest X-ray

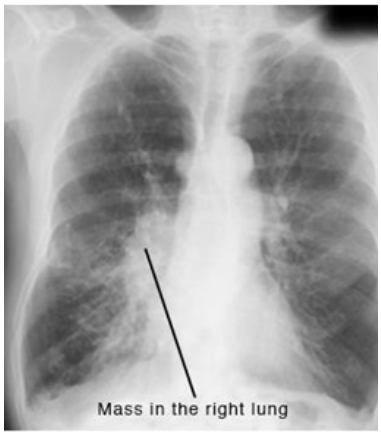

Figure 1.2: Cancer image

CNN-based lung cancer prediction faces indecisive x-ray images because some of the x-ray images are not more detailed and some information may be missing. Indeed, as an adjustment, the gamma correction method is used for obtaining the more detailed information about the images. Unfortunately, in the available dataset, the images were not more detailed and clear, meaning they did not contain much information. In the proposed model, we have used the

gamma correction method to improve the quality and intensity of the image, which also improves the performance of the model. The Gamma correction method was used twice, once with a gamma value > 0 and again with a gamma value 0. Such a gamma correction technique solves the problem of indecisive x-ray images and achieves a better result compared to the other techniques. In addition, the study also shows that it is possible to calculate a heat map showing the predicted location of lung cancer in chest X-ray images.

1.1 ANATOMY OF CHESTX-RAY

Anatomical structure determines the labeled parts of the chest image. The thoracic cavity,

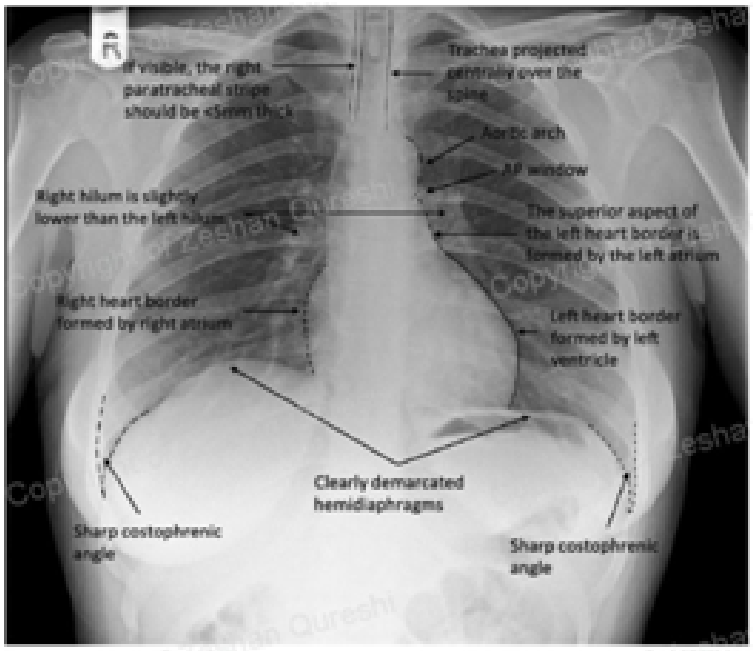

Figure 1.3: Anatomy of Chest X-ray

also known as the chest cavity, is the body's second largest hollow space. It is limited by the ribs, the vertebral segment, and the sternum, or breastbone, and is isolated from the stomach cavity by the stomach, a strong and membranous parcel. The lungs, the middle and lower airways (the tracheobronchial tree), the heart, the vessels that transport blood between the heart and the lungs, the great arteries that bring blood from the heart out into general circulation and the major veins that collect blood for transport back to the heart are all part of it. The pericardium, a fibrous membrane sac that blends with the trunks of the vessels covers the heart.

1.1.1 DIFFERENT GRADES OF LUNGCANCER

Evaluating is a method of partitioning malignant growth cells into bunches dependent on the way that the cells look under a magnifying instrument. This provides us with an idea of how rapidly or gradually the malignant growth may develop and whether it is likely to spread. For most cellular breakdowns in the lungs, there is nothing but a particular reviewing framework specialist's utilization. [3]

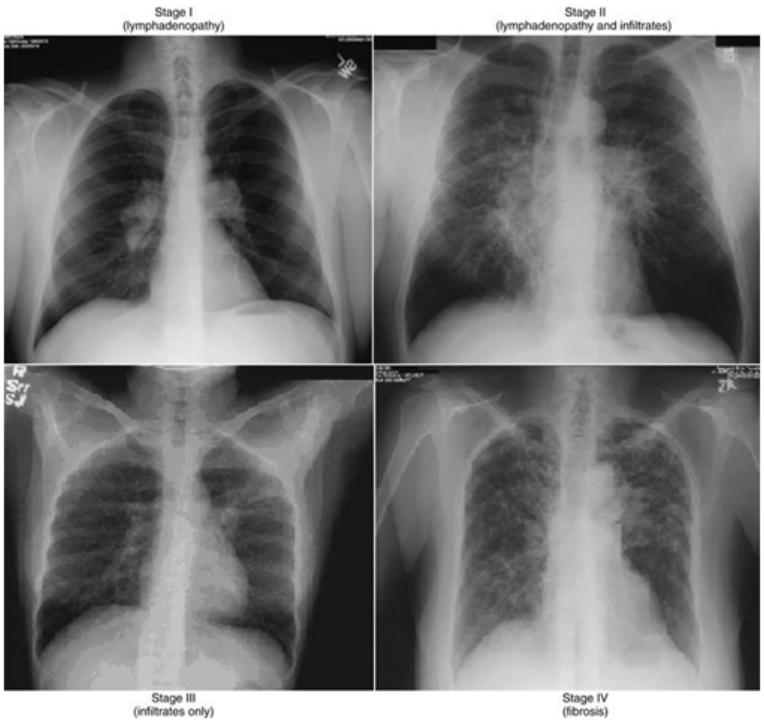

Figure 1.4: Different stages of Lung cancer

Grade 1

The cells look exceptionally like typical cells. They will typically develop slowly and are less likely to spread than higher-grade disease cells. They are called poor quality or lower grade.

Grade 2

The cells look stranger and are bound to spread. This grade is likewise called a decently all-around-separate or moderate grade.

Grade 3 and 4

The cells look extremely unusual, unlike ordinary cells. They will, more often than not, develop Rapidly and are bound to spread. They are called ineffectively separated or "high

grade.[1]

1.2 MOTIVATION

The inspiration for this venture is that around 10 to 15 percent of smokers create cellular breakdown in the lungs in spite of the fact that they frequently pass on from other smoking-related causes like coronary illness, stroke, or emphysema. As indicated by the new study, the worldwide number of smokers keeps on ascending, with smoking causing almost 8 million deaths in 2019, with one in five males dying.[2] A general endurance rate contrasts individuals with a similar kind and phase of disease to individuals in the general populace. By and large, around 60% as logical as individuals who don't have that disease to live for something like 5 years in the wake of being diagnosed? [1]*[3]

1.3 LITERATURE SURVEY

A writing survey is a cycle of summing up, incorporating, and evaluating the writing found because of a writing search. Table 1 gives a short depiction of all the writing audits or foundation studies done prior to executing the undertaking.

Sl.No	TITLE OF PAPER,AUTHORS AND PUBLISHED YEAR	Methodology	Dataset	Results
[4] 1.	Automatic Lung Cancer Prediction from Chest X-ray Images Using the Deep Learning Approach Worawate Ausawalaithon The 2018 Biomedical Engineering International Conference (BMEiCON-2018)	Convolutional neural network (CNN)	JSRT Dataset and ChestX-ray14 Dataset	Accuracy = 74% specificity = 74.96% Sensitivity = 74.68 %
[?] 2.	Lung cancer prediction using machine learning and advanced imaging techniques Timor Kadiret.al.2018	Convolutional neural network (CNN)	2017 lung cancer detection data science bowel (DSB)	AUC-ROC results of 0.85 and 0.87
3.	ediction and Classification of Lung Cancer Using Machine Learning Techniques PragyaChaturvediet.al.,2020	Convolutional neural network (CNN)	LUNA16, Super Bowl Dataset 2016	Accuracy 97.1%, Sensitivity 95.9% Specificity 98.1%
4.	Lung cancer prediction by Deep Learning to identify benign lung nodules MarjoleinA.Heuvelmanset.al., September 2021	Convolutional neural network (CNN)	NLST dataset	Sensitivity 99 %
[5] 5.	Pancreatic Cancer Survival Prediction: A Survey of the State-of the-Art Wilson Bakasaet.al.,30 September 2021	Region Convolution Neural Network (R-CNN)	Cancer Imaging Archive (TCIA) Public Access dataset	Sensitivity 92.1% Accuracy 98.8%, specificity 99.3%
[6] 6 .	A promising step forward for predicting lung cancer ShravyaShetty, M.S.iet.al., May 20, 2019	Convolutional neural network (CNN)	NIH's research dataset	AUC of 94.4 percent

Table 1.1: Table 1 Literature review

Sl.No	TITLE OF PAPER,AUTHORS AND PUBLISHED YEAR	Methodology	Dataset	Results
[7] 7.	Lung Cancer Prediction using Machine Learning Syed SabaRaoofet.al., 23 April 2020	Computer-aided diagnosis(CAD)	LUNA16	Accuracy 82% , AUC about 0.885, AUPRC about 0.837.
[8] 8	Automated abnormality classification of chest radiographs using deep convolutional neural networks Yu-Xing Tang et.al.14 may 2020	Convolutional neural network (CNN)	NIH ChestX-ray 14	Accuracy 94.64±0.45%, Sensitivity 96.50±0.36% Specificity 92.86±0.48%
[9] 9	Weakly supervised learning for classification of lung cytological images using attention-based multiple instance learning Atsushi Teramotoet.al.13 October 2021	AlexNet-like convolutional neural network model	Institutional Review Board of Fujita Health University (IRB number: HM16-155)	Accuracy 0.916
[10] 10	Hybrid deep learning for detecting lung diseases from X-ray images SubratoBharati, et.al. 2020 Jul 4	Convolutional neural network (CNN), vanilla neural network, visual geometry group based neural network (VGG), and capsule network	NIH chest X-ray	Accuracy 67.8%, 69%, 69.5% and 63.8%
[11]				

1.4 RESEARCH GAP

The reported literature has not considered gamma features such that the images are more detailed and clear, which can be applied in training along with images for more accuracy.

1.5 PROBLEM STATEMENT AND OBJECTIVES

An issue articulation may be a brief portrayal of an issue to be tended to or a condition to be progressed upon. Destinations characterise methodologies or usage steps to achieve the distinguished objectives.

1.5.1 PROBLEM STATEMENT

To develop CNN based lung cancer prediction of chest x-ray images.

1.5.2 OBJECTIVES

To explore Gamma corrected Chest X ray images on 121-layer CNN also known as DenseNet-121 for classifying lung cancer.

To achieve mean accuracy, specificity and sensitivity $> 70\%$ (Reference: Automatic Lung Cancer Prediction from Chest X-ray Images Using the Deep Learning Approach)

Perform comparative analysis with literatures reported recently for lung cancer classification.

In this chapter we have discussed about Introduction, Motivation, Literature Survey, Problem Statement and Objectives in next chapter we are discussing about dataset description and dataset preparation.[12]

Chapter 2

DATASET DESCRIPTION AND PREPRATION

In this chapter, we are discussing the description of a dataset utilised and the preparation of a dataset for providing training to the model.

2.1 DATASET DESCRIPTION

The dataset was collected from the kaggle dataset. It is a public dataset from kaggle (COVID-19 Radiography Database). The dataset contains 944 chest X-ray images, including 439 cancerous images and 505 non-cancerous images. The dataset is split into train and test images. The training dataset contains 753 images and the testing dataset contains 188 chest X-ray images.

- The number of images: 944
- Image size: 1989x1489
- Image type: Jpeg (Joint Photographic Experts Group) images.

2.1.1 CANCEROUS IMAGES

The dataset contains 439 cancerous chest X-ray images. X-rays containing cancer will be lighter compared to non-cancerous images because the lungs will be turned to a black colour, and this black colour is from a damaged X-ray. The X-ray containing the chest cancer is shown in Figure 1(b). On cancerous images or X-rays, there will be scar-like tissues present on the chest. This scar-like tissue depends on the different grades of cancer. X-rays with a lower grade usually have a small scar part, which is referred to as "benign X-rays" in medical terms, and X-rays with a higher grade have slightly larger scars than the lower grade, which is referred to as "malignant" in medical terms. Patients with cancer will have more difficulty breathing, as well as other symptoms such as coughing and chest pains.

2.1.2 NON-CANCEROUS IMAGES

The dataset contains 505 normal, non-cancerous chest X-ray images. As shown in figure 1(a), non-cancerous images will look healthy and look brighter compared to X-rays containing cancer, as shown in figure 1(b). There will be no scar like tissues present on X-rays and these X-rays will be red in color. This red color represents the flow of blood. There will be no difficulty in breathing and no symptoms will be found.

2.2 DATASETPREPARATION

The data preparation process normalizes the x-rays by providing various functions or techniques for training the model. After collecting the x-ray dataset, we prepared a dataset for training the model. Firstly, we have taken x-ray images, and then we are converting all the images to gray scale images. Conversion of all the images to grey scale helps to reduce the training time because all converted images will have similar dimensions. Initially, all the images that are X-rays in the dataset were of different sizes, so these images were transformed to 224 X 224 as shown in Figure 3. So all the images were normalized and then we provided them as input to the system.

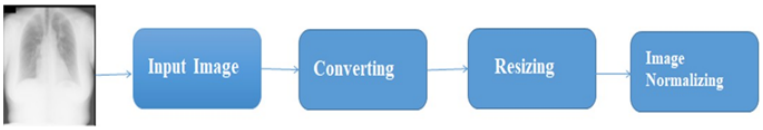

Figure 2.1: Dataset preparation

Data preparation was applied to all images, consisting of the following four steps.

- Step 1: The chest x-ray images were provided as input to the system.
- Step 2: The chest x-ray image is converted to grayscale.
- step 3: Resize all of the images to 224*224 pixels to match the model's input.
- Step 4: Normalizing image colour based on the mean and standard deviation of the ImageNet training set.

The various functions used while pre-processing the chest X-ray images meet the features of input to the model.

CVTCOLOR

cv2.cvtColor() strategy is utilized to change over an picture from one colour space to another. There are more than 150 colour-space change strategies accessible in OpenCV.

RESIZE

Image resizing is vital when we have to increment or diminish the overall number of pixels, though remapping will happen when we are rectifying for focal point mutilation or turning an image.

NORMALIZING

Picture Normalization could be a process in which we change the extent of pixel escalated values to make the picture more recognizable or ordinary to the faculties, thus the term normalization.

In this chapter we have discussed about dataset description and dataset preparation in next chapter we are discussing softwarerequirement specifications.

Chapter 3

SOFTWARE REQUIREMENTS SPECFICATION

In this chapter, we are discussing computer vision libraries and software requirement specifications.

3.1 SOFTWARE REQUIREMENTGATHERING

Python-based computer vision and deep transfer learning libraries will be exploited for the development and experimentation of the project. Software: Anaconda, Jupyter, Python.

3.2 COMPUTER VISION AUGMENTATIONLIBRARIES

The list and explanation of libraries installed during the implementation of the project.

TENSORFLOW

TensorFlow is a free and open-source software library for machine learning and artificial intelligence. Tensorflow is used for importing all keras related libraries, like keras layers, keras preprocessors, and keras applications.

KERAS

Keras is an open-source software library that provides a Python interface for artificial neural networks. It is used for importing training models like the Inception model, DenseNet121 model, Lambda function, Dropout methods, Average pooling method, preprocessing models, and for generating image data.

SKLEARN

Scikit-learn (formerly scikits.learn and also known as sklearn) is a free software machine learning library for the Python programming language. Sickit learn or sklearn is used for applying the confusion matrix and ROC (Receiver Characteristic Operating Curve).

SEABORN

The Seaborn library is used for the visualisation of images in heatmaps. The Seaborn library is used for the visualisation of images in heatmaps.

NUMPY

NumPy is the elemental bundle for logical computing in Python. It is used for retrieving the arrays, like for calling the array to display all the images.

MATPLOTLIB

Matplotlib may be a plotting library for the Python programming language and its numerical number-juggling development, NumPy. The Matplotlib library is used for plotting the graphs.

CV2

OpenCV is a great tool for image processing and performing computer vision tasks. A library is used for displaying the images.

CV2.IMREAD

Cv2.imread is used for displaying the images by reading the specified path

CVTCOLOR

Initially all the images in the dataset All the images were transformed into grey images using the CvtColorfunction.

RESIZE

Initially all the images in the dataset where of size 1989 X 1489 so we have resized all the images 224 X 224 using cv2resize function.

APPEND

The x-rays where labelled like cancerous and non-cancerous and then these x- rays have been appended using cv2.append function for visualizing and training the model for prediction.

GLOB

The glob module finds all the pathnames matching a specified pattern according to the rules used by the UNIX shell, although results are returned in arbitrary order. It is used for declaring the path names for retrieving the images.

In this chapter we have discussed the software requirements used in the project and the Python libraries imported in the next chapter. We are discussing the proposed methodology.

Chapter 4

METHODLOGY

In this chapter, we'll go through the details of the proposed system's detailed design and implementation. The original chest X-ray image with Gamma correction value images where

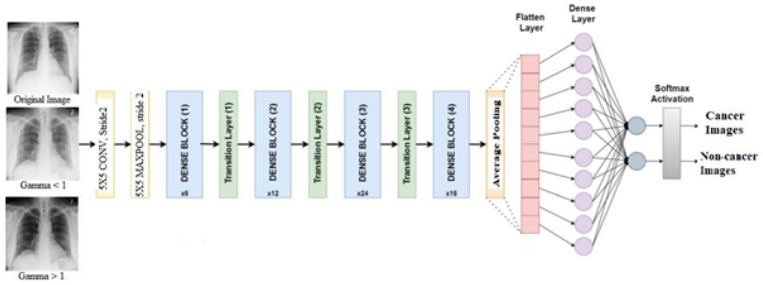

Figure 4.1: Detailed Designs

Gamma<1 and Gamma > 1 images are given input to the system. The images are trained on the Densenet121 model with 5X5 convolutional layers and 2 strides, and the Maxpool layer with 5X5 down samples along with 2 strides. The dense net model has four dense blocks [6, 12, 24, and 16] along with each of the transition layers. Since each thick piece will increment the number of channels, including how numerous of them will lead to a too complex show. A moving layer is utilized to control the complexity of the demonstration. It reduces the number of channels by utilizing the 11 convolutional layer and dividing the height and width of the normal pooling layer by a factor of two, thereby reducing the complexity of the demonstration. It decreases the number of channels by utilizing the 1×1 convolutional layer and parts the height and width of the normal pooling layer with a walk of 2, thus decreasing the complexity of the show.

Then, using the softmax activation function, the model predicts that either the x-ray has cancer or not. Firstly, the dataset was trained with the inceptionV3 model on the imageNet dataset, where we achieved an accuracy of 0.87, an F1 score of 0.89, a precision score of 0.93, and a recall of 0.85 trained on 20 epochs. Finally, we achieved a receiver operating characteristic curve (ROC) of 0.88. Secondly, the dataset was trained with the Densenet121 model on the imageNet dataset, where we achieved an accuracy of 0.86, an F1 score of 0.82, a precision score of 0.79, and a recall of 0.69 trained on 20 epochs. Finally, we achieved a receiver operating characteristic curve (ROC) of 0.99. Gamma < 0.8 and Gamma > 1.5

on imageNet dataset where we achieved the accuracy 0.89 and 0.88, F1 score 0.87 and 0.83, precision score 0.95 and 0.98 recall 0.81 and 0.72 trained on 20 epochs. Finally we achieved the receiver operating characteristic curve (ROC) as 0.98 and 0.99respectively.

4.1 INCEPTION MODEL

Inception v3 may be a convolutional neural network organised to help in picture investigation and protest location, and it began as a module for Googlenet. It is the third version of Google's Initiation Convolutional Neural Organize, initially presented amid the ImageNet Acknowledgment Challenge. Inceptionv3's design goal was to allow for more complex systems while keeping the number of parameters from growing too large: it has "less than 25 million parameters," compared to AlexNet's 60 million.Just as ImageNet can be thought of as a database of classified visual objects, the beginning makes a difference in the classification of objects within the world of computer vision. Inceptionv3 engineering has been reused in numerous diverse applications, frequently utilising "pre-trained" from ImageNet. One such use is in life sciences, where it helps in the research of leukemia.[13] Firstly, we trained the

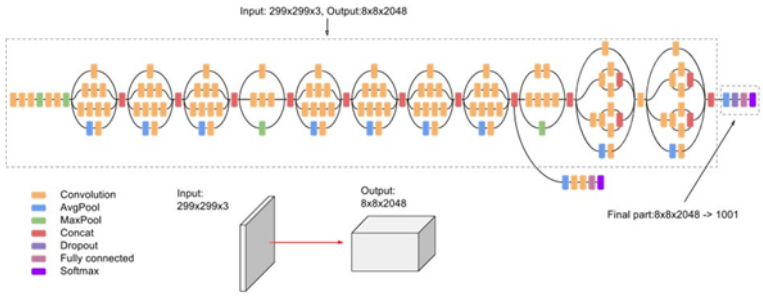

Figure 4.2: Inception V3 model

dataset on the InceptionV3 model, which is again a convolutional neural network. We achieved an accuracy of 0.88. F1 score, Precision, Recall, and Support at 0.95, 0.72, 0.82 and 87, respectively, which is shown in Figure 6 classification report of the inceptionV3 model.

	precision	recall	f1-score	support
0	0.95	0.72	0.82	87
1	0.80	0.97	0.88	101
accuracy			0.86	188
macro avg	0.88	0.85	0.85	188
weighted avg	0.87	0.86	0.85	188

Figure 4.3: Classification report of inceptionv3 model

4.2 DENSENET121 MODEL

In a conventional feed-forward convolutional neural network (CNN), each convolutional layer but the primary one (which takes within the input) gets the yield of the previous convolutional layer and produces a yield including the outline that's at that point passed on to the next convolutional layer. Hence, for 'L' layers, there are 'L' coordinate associations; one between each layer and the next layer. We once more prepared the dataset on Densenet121 to demonstrate that it could be a convolutional neural organization. We were able to achieve 0.88 precision.F1

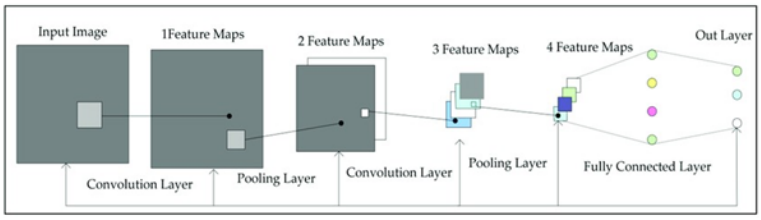

Figure 4.4: Densenet121 Model

score, Accuracy, and Review were as low as 0.92, 0.79, 0.85, and 100, respectively, as shown in Figure 8 Classification Report of the densenet121 model.

	precision	recall	f1-score	support
0	0.79	0.92	0.85	87
1	0.92	0.79	0.85	101
accuracy			0.85	188
macro avg	0.86	0.86	0.85	188
weighted avg	0.86	0.85	0.85	188

Figure 4.5: Classification report Densenet121 Model

4.3 GAMMA CORRECTION METHOD

This method is a nonlinear filter which adjusts the image brightness based on the predefined Gamma parameter. For a considered image, the general form transformed gamma correction (TGC) is calculated as follows:

TGC= I_M (I_i /I_M)^γ

where, I_i describes the intensity of the image, I_M describes the maximum value of the intensity in the input image, and is a tunable parameter in the interval (0,). In the equation above, the Gamma parameter changes the intensity of the pixel in the image. If =1, it does not perform any changes on the input image. However, if <1, it enhances the brightness, and if >1, it decreases the image brightness; i.e., the selection of the Gamma directly affects the image intensity. Hence, it is essential to select an optimal value for the Gamma parameter. We have applied a gamma correction method on DenseNet121 model and inception model where we have set gamma > 0 that is gamma $= 1.5$ and we have set gamma < 0 that isgamma $=$ 0.8.

Figure 4.6: Inputimage

Figure 4.7: Gamma<0

Figure 4.8: Gamma >0

4.4 TRAIN TEST SPLIT METHOD

We have used a train-test split method which randomly splits the dataset. $\text{train}_t est_s plitmaybeaworkinSkl$
$forpreparinginformationandfortestingdata.Withthiswork, youdonotoughttoseparatethedatasetphysic$
$rayimagesandtestingdatasetcontains188chestX-rayimages.$[15]

4.5 AUGMENTATION METHOD

The enlargement strategies utilized within the show is Turn run, Width move extend, Stature Move run and Level flip strategies as 20, 0.2, and 0.2 an genuine respectively

4.5.1 ROTATIONRANGE

A source picture is irregular turned counter clockwise by 20 degrees position in outline. Outstandingly, for location of cancer in X-rays, the bounding box is overhauled to envelop the coming about object.

4.5.2 WIDTH SHIFTRANGE

The X-rays is uprooted by 0.2 on a division of the generally width.

4.5.3 HEIGHT SHIFTRANGE

The picture is displaced by 0.2 on a fraction of the overall height.

4.5.4 HORIZONTALFLIP

Horizontal shifts are interior changes that influence the input x- pivot values and move the work cleared out or right. Combining the two sorts of shifts will cause the chart of a work to move up or down and right or cleared out. Even flip was set to true.

4.6 LABELBINARIZER

Binarize labels is a one-vs-all fashion.A few relapse and double classification calculations are accessible in scikit-learn.Using label Binarizer we are classifying the cancerous and non-cancerous chest X-rays where our dataset contains 944 chest X-ray images in total.

4.7 LOSS FUNCTION AND OPTIMZER

Loss is a prediction error encountered in a Neural Net. And the strategy to calculate the loss is called Loss Work. A loss work we have utilized is Categorical cross entropy and optimizer work is adam. Categorical cross entropy loss work is utilized for classifying cancer and non-cancer pictures in a dataset and to expel blunder from a Neural arrange after the classification. Adam optimizer includes a combination of two slope plummet strategies: Momentum: This calculation is utilized to quicken the angle plunge calculation by taking into thought the 'exponentially weighted average' of the angles. Utilizing midpoints makes the Calculation merges towards the minima in a quicker pace.

Where ti and si are the ground truth and the CNN score for each class i in C. As usually an activation function Softmax is applied to the scores before the CE Loss computation, we write f (si) to refer to the activations. In a binary classification problem, where C =2, the Cross

$$CE = -\sum_{i}^{C} ti \log s_i$$

Entropy Loss can be defined also as Where it's assumed that there are two classes: C1C1 and

$$CE = -\sum_{i=1}^{c'=2} t_i log(s_i) = -t_1 log(s_1) - (1 - t_1) \log (1 - s_1)$$

C2C2. t1t1 [0, 1] and s1s1 are the groundtruth and the score for C1C1, and t2=1t1t2=1t1 and s2=1s1s2=1s1 are the groundtruth and the score for C2C2. That is the case when we split a Multi-Label classification problem in C binary classification problems.

4.8 CLASS ACTIVATION MAPPINGS(CAMS)

Softmax work is utilized as the enactment work within the yield layer of neural organizes models that anticipate an x-ray picture contains cancer or not. Optimizer may be a work adjusts the qualities of the neural organize, such as weights and learning rate. In this way, it makes a difference in diminishing the in general loss and moves forward the exactness. where

$$\sigma(\vec{z})i = \frac{e^{zi}}{\sum_{j=1} K\ e^{zj}}$$

all the zi values are the components of the input vector and can take any genuine esteem. The term on the foot of the equation is the normalization term which guarantees that all the yield values of the work will entirety to 1, hence constituting substantial likelihood dispersion.

In this section we have discussed about detailed description of proposed model and the models used, train-test split method, augmentation methods, loss function, optimizer method and class activation function and in upcoming chapter we are discussing implementation details.

Chapter 5

IMPLEMENTATION

In this section will discuss the training, testing, and prediction methodologies for implementation.

5.1 TRAININGMETHOD

We trained the dataset on two different models: the inception model and the densenet121 model, and then we applied the gamma correction method. Firstly, the augmentation method was applied and trained on 20 epochs. An epoch implies preparing the neural organ with all the preparing information for one cycle. The training method was done using the train-test-split method, where it randomly splits the dataset. The training accuracy we achieved after training on the Inceptionv3 model was 0.88 per cent, which is shown in Figure 9, and on training the densenet121 model, we achieved a 0.88 per cent training accuracy for the model, which is shown in Figure 10.

```
Epoch 1/20
23/23 [==============================] - 115s 5s/step - loss: 3.9399 - accuracy: 0.6795 - val_loss: 0.8219 - val_accuracy: 0.7979
Epoch 2/20
23/23 [==============================] - 104s 4s/step - loss: 0.8707 - accuracy: 0.8138 - val_loss: 0.6009 - val_accuracy: 0.8670
Epoch 3/20
23/23 [==============================] - 105s 5s/step - loss: 0.8321 - accuracy: 0.8165 - val_loss: 1.1184 - val_accuracy: 0.8245
Epoch 4/20
23/23 [==============================] - 105s 4s/step - loss: 1.2147 - accuracy: 0.7952 - val_loss: 3.1168 - val_accuracy: 0.7021
Epoch 5/20
23/23 [==============================] - 108s 5s/step - loss: 1.8972 - accuracy: 0.7912 - val_loss: 4.2630 - val_accuracy: 0.5479
Epoch 6/20
23/23 [==============================] - 106s 5s/step - loss: 1.4040 - accuracy: 0.8271 - val_loss: 0.9272 - val_accuracy: 0.8138
Epoch 7/20
23/23 [==============================] - 105s 5s/step - loss: 0.7029 - accuracy: 0.8803 - val_loss: 0.7608 - val_accuracy: 0.8670
Epoch 8/20
23/23 [==============================] - 106s 5s/step - loss: 0.7631 - accuracy: 0.8737 - val_loss: 0.7868 - val_accuracy: 0.8564
Epoch 9/20
23/23 [==============================] - 105s 4s/step - loss: 0.7973 - accuracy: 0.8723 - val_loss: 1.3854 - val_accuracy: 0.8245
Epoch 10/20
23/23 [==============================] - 105s 4s/step - loss: 0.8303 - accuracy: 0.8830 - val_loss: 1.2572 - val_accuracy: 0.7872
Epoch 11/20
23/23 [==============================] - 105s 5s/step - loss: 0.9145 - accuracy: 0.8551 - val_loss: 1.8059 - val_accuracy: 0.7287
Epoch 12/20
23/23 [==============================] - 105s 5s/step - loss: 1.2517 - accuracy: 0.8431 - val_loss: 2.1825 - val_accuracy: 0.7926
Epoch 13/20
23/23 [==============================] - 106s 5s/step - loss: 1.0496 - accuracy: 0.8750 - val_loss: 1.1286 - val_accuracy: 0.8723
Epoch 14/20
23/23 [==============================] - 110s 5s/step - loss: 1.0253 - accuracy: 0.8617 - val_loss: 1.3050 - val_accuracy: 0.8085
Epoch 15/20
23/23 [==============================] - 107s 5s/step - loss: 0.7955 - accuracy: 0.8816 - val_loss: 0.7241 - val_accuracy: 0.8617
Epoch 16/20
23/23 [==============================] - 106s 5s/step - loss: 0.6413 - accuracy: 0.8949 - val_loss: 3.5065 - val_accuracy: 0.6170
Epoch 17/20
23/23 [==============================] - 109s 5s/step - loss: 1.6888 - accuracy: 0.8165 - val_loss: 2.5595 - val_accuracy: 0.8085
Epoch 18/20
23/23 [==============================] - 105s 5s/step - loss: 1.3270 - accuracy: 0.8670 - val_loss: 0.8083 - val_accuracy: 0.8830
Epoch 19/20
23/23 [==============================] - 106s 5s/step - loss: 0.7546 - accuracy: 0.8949 - val_loss: 0.8148 - val_accuracy: 0.8723
Epoch 20/20
23/23 [==============================] - 105s 4s/step - loss: 0.7433 - accuracy: 0.8870 - val_loss: 1.0829 - val_accuracy: 0.8564
```

Figure 5.1: Training epochs of inception model

```
Epoch 1/20
23/23 [==============================] - 108s 5s/step - loss: 1.0201 - accuracy: 0.8564 - val_loss: 0.9723 - val_accuracy: 0.8245
Epoch 2/20
23/23 [==============================] - 103s 4s/step - loss: 0.8721 - accuracy: 0.8843 - val_loss: 0.6548 - val_accuracy: 0.8511
Epoch 3/20
23/23 [==============================] - 104s 4s/step - loss: 0.8299 - accuracy: 0.8923 - val_loss: 0.7209 - val_accuracy: 0.8830
Epoch 4/20
23/23 [==============================] - 103s 4s/step - loss: 0.9708 - accuracy: 0.8936 - val_loss: 0.7896 - val_accuracy: 0.8670
Epoch 5/20
23/23 [==============================] - 105s 5s/step - loss: 0.8142 - accuracy: 0.8843 - val_loss: 1.1135 - val_accuracy: 0.8883
Epoch 6/20
23/23 [==============================] - 104s 4s/step - loss: 1.5205 - accuracy: 0.8590 - val_loss: 1.4090 - val_accuracy: 0.8564
Epoch 7/20
23/23 [==============================] - 105s 5s/step - loss: 1.0698 - accuracy: 0.8737 - val_loss: 0.7420 - val_accuracy: 0.8830
Epoch 8/20
23/23 [==============================] - 105s 4s/step - loss: 0.7231 - accuracy: 0.9003 - val_loss: 1.0587 - val_accuracy: 0.8777
Epoch 9/20
23/23 [==============================] - 106s 5s/step - loss: 0.8376 - accuracy: 0.9056 - val_loss: 1.5163 - val_accuracy: 0.8404
Epoch 10/20
23/23 [==============================] - 105s 4s/step - loss: 1.1702 - accuracy: 0.8604 - val_loss: 1.1029 - val_accuracy: 0.8777
Epoch 11/20
23/23 [==============================] - 105s 4s/step - loss: 1.4310 - accuracy: 0.8577 - val_loss: 2.5426 - val_accuracy: 0.7287
Epoch 12/20
23/23 [==============================] - 105s 4s/step - loss: 1.5748 - accuracy: 0.8524 - val_loss: 0.9023 - val_accuracy: 0.8936
Epoch 13/20
23/23 [==============================] - 105s 4s/step - loss: 1.5248 - accuracy: 0.8630 - val_loss: 1.4051 - val_accuracy: 0.8351
Epoch 14/20
23/23 [==============================] - 105s 4s/step - loss: 1.0177 - accuracy: 0.8910 - val_loss: 1.1163 - val_accuracy: 0.8351
Epoch 15/20
23/23 [==============================] - 105s 4s/step - loss: 0.6251 - accuracy: 0.9082 - val_loss: 1.1250 - val_accuracy: 0.8936
Epoch 16/20
23/23 [==============================] - 104s 4s/step - loss: 0.9582 - accuracy: 0.8896 - val_loss: 2.5237 - val_accuracy: 0.8138
Epoch 17/20
23/23 [==============================] - 106s 5s/step - loss: 1.0404 - accuracy: 0.8856 - val_loss: 1.1334 - val_accuracy: 0.8404
Epoch 18/20
23/23 [==============================] - 122s 5s/step - loss: 1.0125 - accuracy: 0.8949 - val_loss: 0.9409 - val_accuracy: 0.9043
Epoch 19/20
23/23 [==============================] - 105s 5s/step - loss: 0.8447 - accuracy: 0.9043 - val_loss: 1.5570 - val_accuracy: 0.8617
Epoch 20/20
23/23 [==============================] - 107s 5s/step - loss: 1.2634 - accuracy: 0.8856 - val_loss: 1.2571 - val_accuracy: 0.8511
```

Figure 5.2: Training epochs on densenet121 model

5.2 TESTINGMETOD

After preparing the demonstrate we provide the show for testing as we have utilized train-test-split strategy it arbitrarily parts the test set it takes 188 as a testing esteem. The test precision we have connected a perplexity lattice.

5.2.1 CONFUSIONMATRIX

A confusion matrix depicts the execution of a classification show on a set of test information for which the genuine values are known. The perplexity network comprises of four essential characteristics (numbers) that are utilized to characterize the estimation measurements of the classifier. These four numbers are:

1.TRUE POSITIVE(TP)

TP represents the number of patients who have been appropriately classified to have cancer. The Genuine positive we gotten for the initiation demonstrate without the gamma adjustment strategy is 85, essentially for the initiation show with gamma < 1 we gotten TP of 85, and at long last for gamma redress > 1 we gotten TP of 99. Essentially for Densenet121 the Genuine positive we gotten without the gamma rectification strategy is 85, essentially for the densenet121 show with gamma < 1 we gotten TP of 94, and at last for gamma correction $>$ 1 we gotten TP of 95.

2.FALSE POSITIVE (FP)

FP represents the number of misclassified patients with the disease but actually they are healthy. FP is also known as a Type I error. The False positive we obtained for the inception model without the gamma correction technique is 7, with gamma correction < 1 we obtained FP of 10, and lastly for gamma correction > 1 we obtained FP of 27.Similarly for Densenet121 the False positive we obtained 4 without the gamma correction technique is 6, similarly for the densenet121 model with gamma < 1 we obtained FP of 94, and finally for gamma correction > 1 we obtained FP of 16.

3.TRUE NEGATIVE

TN represents the number of accurately classified patients who are sound. Misclassified patients with the illness but really they are sound. The Genuine Negative we gotten for the initiation demonstrate without the gamma rectification strategy is 80, with gamma adjustment < 1 we gotten TN of 58, and finally for gamma rectification > 1 we gotten TN of 59.Similarly for Densenet121 the Genuine Negative we gotten without the gamma redress strategy is 83, essentially for the densenet121 show with gamma < 1 we gotten TN of 58, and in conclusion for gamma redress > 1 we gotten TN of 59.

4.FALSE NEGATIVE

FN represents the number of patients misclassified as sound but really they are enduring from the illness. FN is additionally known as a Sort II blunders. The Wrong Negative we gotten for the initiation demonstrate without the gamma rectification strategy is 16, with gamma redress < 1 we gotten FN of 3, and in conclusion for gamma rectification > 1 we gotten FN of 3.Similarly for Densenet121 the Untrue Negative we gotten without the gamma rectification strategy is 39, with gamma < 1 we gotten TN of 7, and in conclusion for gamma rectification > 1 we gotten FN of 7.

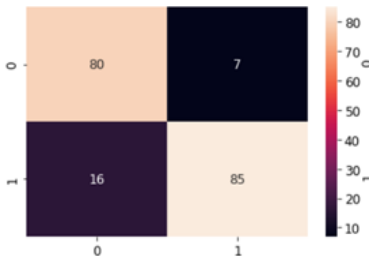

Figure 5.3: Inception model without gamma correction

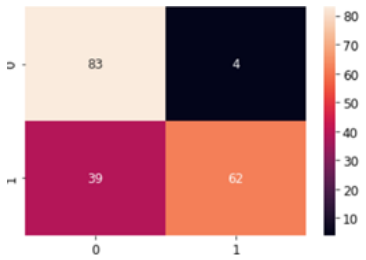

Figure 5.4: Densenet121 model without Gamma correction

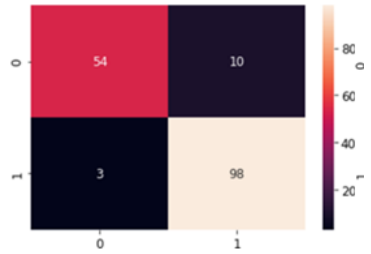

Figure 5.5: Inception model with gamma gamma correction< 1

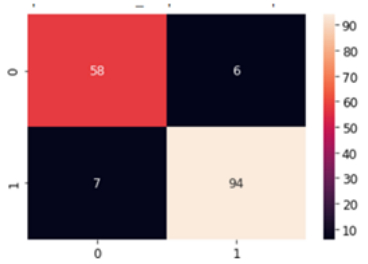

Figure 5.6: Densenet121model with gamma correction< 1

Figure 5.7: Inception model with gamma correction > 1

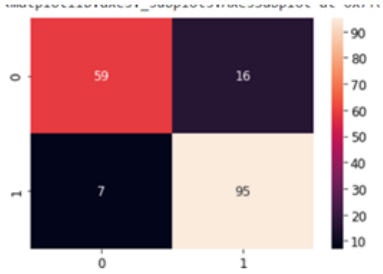

Figure 5.8: Densenet121 model with gamma correction > 1

Table 2 Values of Confusion matrix

Model	Gamma Function	TP	FP	TN	FN
Inception model	Without Gamma Function	85	7	80	16
	With Gamma correction < 1	98	10	54	3
	With Gamma correction > 1	99	27	48	3
Densenet121 model	Without Gamma Function	62	4	83	39
	With Gamma correction < 1	94	6	58	7
	With Gamma correction>1	95	16	59	7

Performance metrics of an algorithm are accuracy, precision, recall, and F1 score, which are calculated on the basis of the above-stated TP, TN, FP, and FN.

ACCURACY

Accuracy of an algorithm is represented as the ratio of correctly classified cancer X-rays (TP+TN) to the total number of X-rays. (TP+TN+FP+FN).

Accuracy = (TP) + (FP)/ (TP) + (FP) + (TN) + (FN)

By training our model we obtained testing accuracy of the inception model without gamma correction is 0.77, with gamma correction < 0.92, with gamma correction > 1 is 0.83. Similarly for densenet121 model the testing accuracy without gamma correction 0.77, with gamma correction < 1 is 0.92 and with gamma correction > 1 is 0.87.

PRECISION

Precision of an algorithm is represented as the ratio of correctly classified patients with the cancer (TP) to the total patients predicted to have the cancer (TP+FP).

PRECISION = TP/TP+FP

The accuracy we got for the beginning show without gamma adjustment for cancerous X-rays is 0.92 and for non-cancerous X-rays is 0.83. With gamma redress<1 for cancerous chest X-rays is 0.91 and for non-cancerous chest X-rays we got 0.95. With gamma adjustment > 1 we got for cancerous chest X-rays is 0.79 and for non-cancerous X-rays we got 0.84. Similarly, densenet121 demonstrated that without gamma adjustment, we got 0.94 for cancerous X-rays and 0.68 for non-cancerous X-rays. With gamma correction 1, we got 0.94 for cancerous chest X-rays and 0.89 for non-cancerous chest X-rays. With gamma correction > 1, we got 0.86 and 0.89 for non-cancerous X-rays.

RECALL

Recall metric is characterized as the proportion of accurately classified unhealthy patients (TP) separated by add up to number of patients who have really the illness. The discernment behind review is how numerous patients have been classified as having the malady. Review is additionally called as sensitivity. RECALL = TP/TP+FN

The recall we obtained for the inception model without gamma correction for cancerous X-rays is 0.94 and for non-cancerous X-rays is 0.68. With gamma correction 1, < 1 for cancerous chest X-rays and for non-cancerous chest X-rays we obtained 0.91. With gamma correction $>$ 1 we obtained 0.97 for cancerous chest X-rays and for non-cancerous X-rays we obtained 0.64. Correspondingly, for the densenet121 model without gamma correction for cancerous X-rays,

we obtained 0.95 and for non-cancerous X-rays, we obtained 0.61. With gamma correction < 1 for cancerous chest X-rays, we obtained 0.91. With gamma correction > 1 we obtained 0.93. For non-cancerous chest X-rays, we obtained 0.79.

F1 SCORE

F1 score is additionally known as the F Degree. The F1 score states the harmony between the accuracy and the review. F1SCORE = 2* precision*recall/precision +recall

The F1 score we obtained for the inception model without gamma correction for cancerous X-rays is 0.88 and for non-cancerous X-rays is 0.87. With gamma correction < 1 the cancerous chest X-rays were 0.94 and for non-cancerous chest X-rays we obtained 0.81, with gamma correction > 1 the cancerous chest X-rays were 0.87 and for non-cancerous X-rays we obtained 0.76. Correspondingly, for the densenet121 model without gamma correction for cancerous X-rays, we obtained 0.74 and for non-cancerous X-rays we obtained 0.79. With gamma correction 1, < 1 for cancerous chest X-rays and for non-cancerous chest X-rays we obtained 0.91. With gamma correction > 1, we obtained 0.89 for cancerous chest X-rays and for non-cancerous X-rays we obtained 0.84.

5.3 PREDICTION METHOD

Predicting whether a chest X-ray given as an input is a cancerous one or not. We have predicted for both the models, that is, for the inception model and the densenet121 model.

5.3.1 The prediction results of inception model

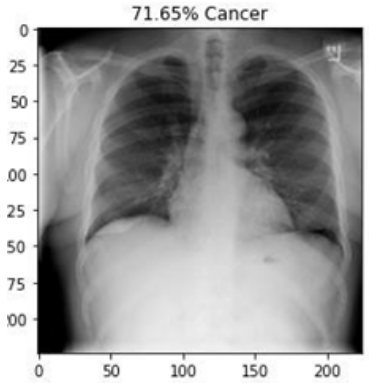

Figure 5.9: Cancer Prediction 71.65%

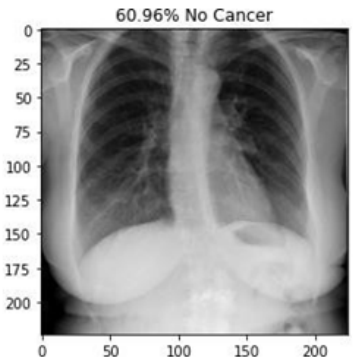

Figure 5.10: No Cancer Prediction 60.96%

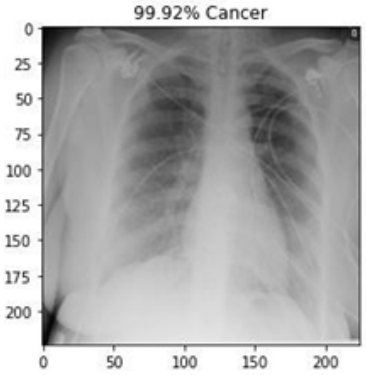

Figure 5.11: 99.92% cancer predictions

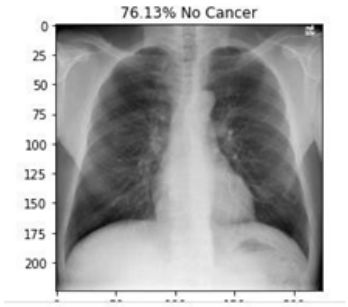

Figure 5.12: 76.13%No Cancer Prediction

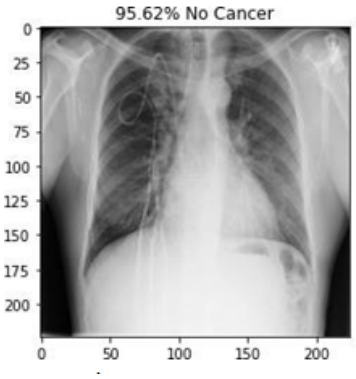

Figure 5.13: 100% Cancer

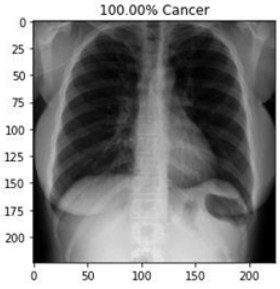

Figure 5.14: 95.62% No Cancer

Without gamma correction, the Inception model predicts a cancerous X-ray at 71.65% and a non-cancerous X-ray at 60.96%, as shown in figures 11 and 20. Figures 21 and 22 show that using the Inception model with gamma correction 1, cancerous X-rays are predicted to be 71.65% and non-cancerous X-rays are predicted to be 60%. Figures 23 and 24 show that with gamma correction > 1, cancerous X-rays are predicted to be 100% and non-cancerous X-rays Are predicted to be 95.62%.

5.3.2 The predictions result of densenet121model.

Without gamma correction, the Densenet121 model predicts a cancerous X-ray at 100% and a non-cancerous X-ray at 63.44%, which is shown in figures 25 and 26. Figures 27 and 28 show that using the Densenet121 model with gamma correction < 1, cancerous X-rays are predicted is 100% and non-cancerous X-rays are predicted to be 99.93%. Figures 29 and 30 show that with gamma correction > 1, cancerous X-rays are predicted to be 100% and non-cancerous X-rays are predicted as100%.

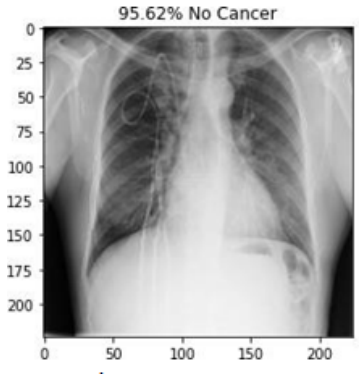

Figure 5.15: Cancerpredicted100%

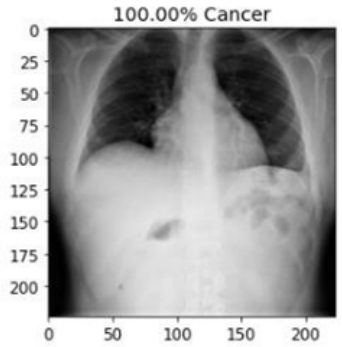

Figure 5.16: No cancer predicted63.44%.

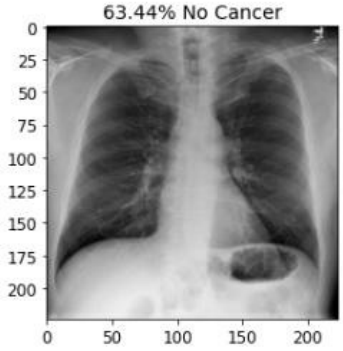

Figure 5.17: 100% Cancer prediction

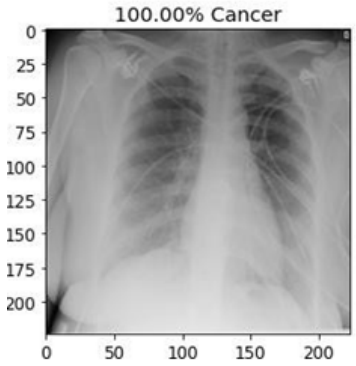

Figure 5.18: 99.93% No Cancer prediction.

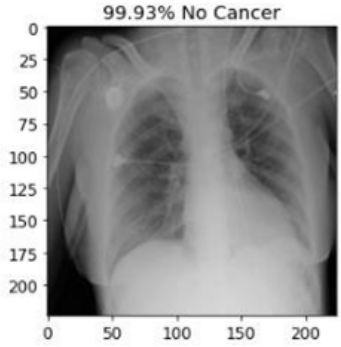

Figure 5.19: 100%CancerPrediction

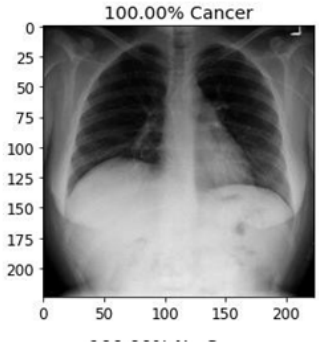

Figure 5.20: 99.93% No Cancer prediction.

In this section we have discussed about training method, testing method and prediction method the results we obtained by the model.

Chapter 6

RESULTS AND DICUSSION

This section explains the ROC Curve model's and graph's outcomes.

6.1 ROC CURVE MODEL

Plotting the true positive rate (TPR) against the false positive rate (FPR) at various threshold values yields the ROC curve. Sensitivity, recall, and probability of detection are almost all terms that describe the true-positive rate. The probability of false alarm [9] is also known as the false-positive rate, and it can be approximated as (1 specificity).A plot of the power as a function of the Type I Error of the decision rule is also called as a power plot (when the performance is calculated from just a sample of the population, it can be thought of as estimators of these quantities). The Receiver characteristic of Operating Curve (ROC) for inception models is shown in Figure 23, 24 and 25.
The figure 23 shows ROC Curve of Inception model without gamma correction where ROC curve is 0.82. In figure 24 the ROC Curve for gamma correction < 1 with inception model

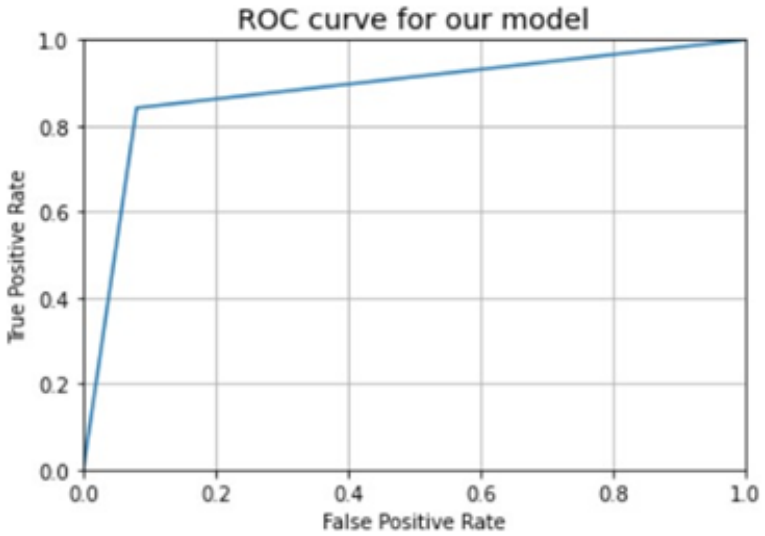

Figure 6.1: ROC curve of inception model without gamma correction

is 0.98. In figure 25 the ROC Curve for gamma correction > 1 with inception model is 0.99.

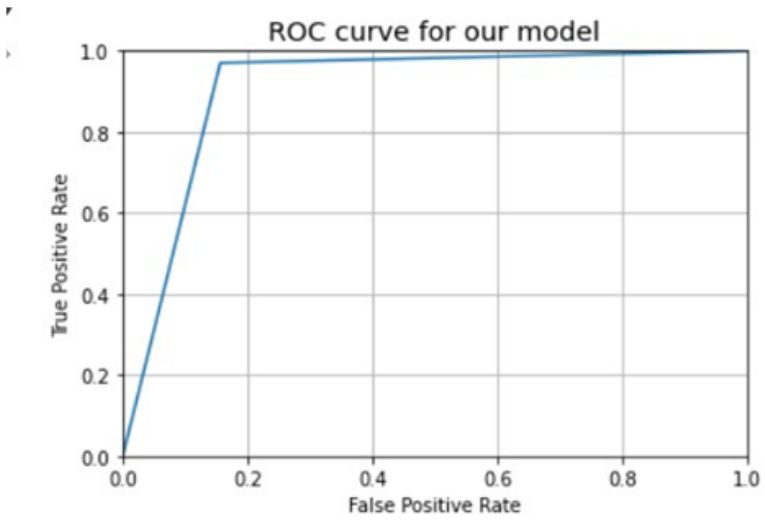

Figure 6.2: ROC curve of inception model with gamma correction < 1

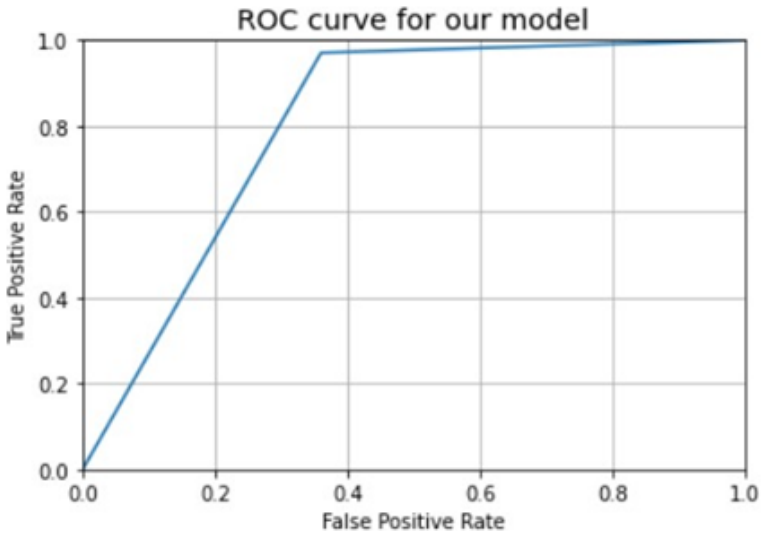

Figure 6.3: ROC Curve of inception model with gamma > 1

The Receiver characteristic of Operating Curve (ROC) for densenet121 models is shown in Figure 26, 27 and 28.

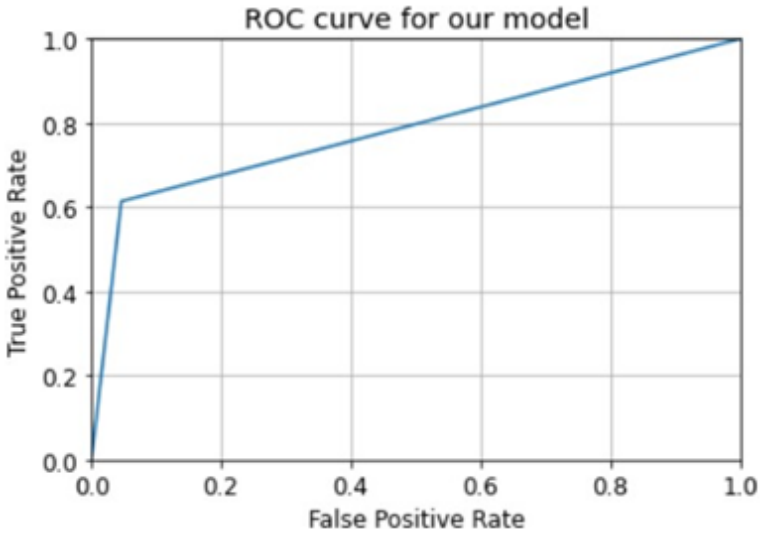

Figure 6.4: ROC Curve of Densenet121 model without gammacorrection

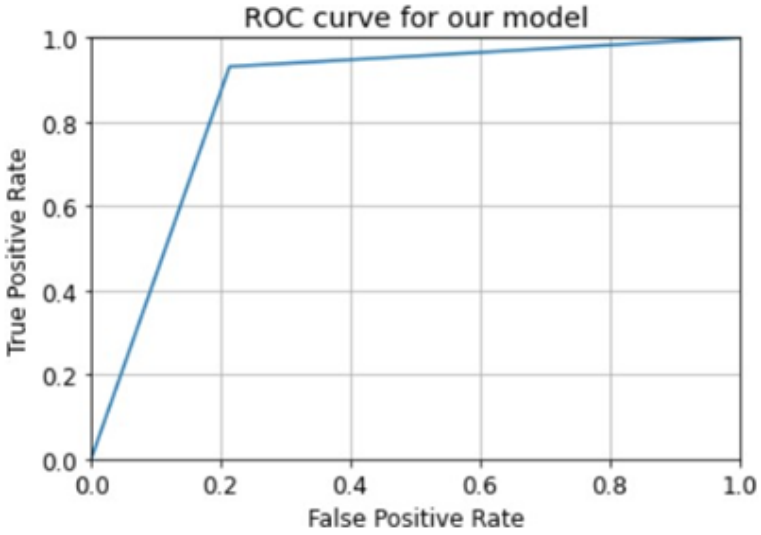

Figure 6.5: ROC Curve of Densenet121 model with gamma correction <1

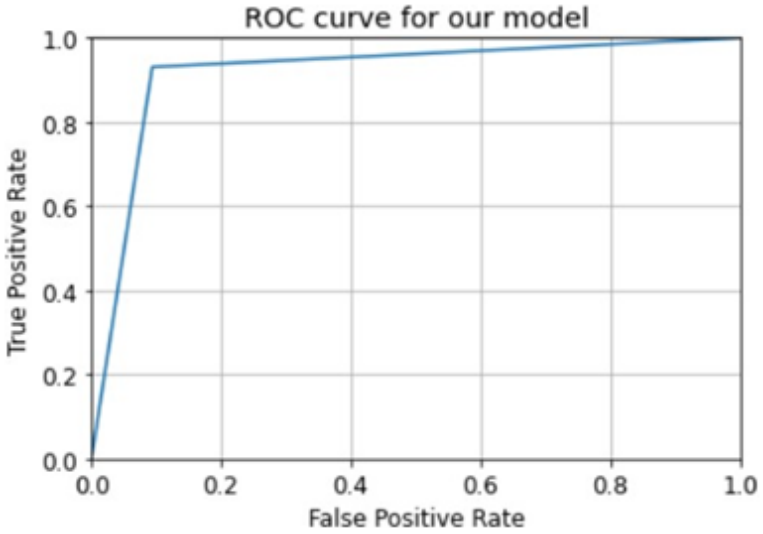

Figure 6.6: ROC Curve of Densenet121 model with gamma correction <1

6.2 COMPARSIONTABLE

Sensitivity, Specificity, and f1 Score comparisons between the Inception model and the Densenet121 model.

6.2.1 Without Gamma Correction for 20epochs

Training data size: 752 Testing data size: 188 Performance of Testing

Model	F1 score	Sensitivity	Specificity	Epochs
Inception	81	83	65	20
Densenet-121	80	77	72	20

With Gamma Correction (Gamma $>$ 1)

Training data size: 703 Testing data size: 177 Performance of Testing

Model	F1 score	Sensitivity	Specificity	Epochs
Inception	92	71	91	20
Densenet-121	83	54	101	20

With Gamma Correction (Gamma $<$ 1)

Training data size: 658 Testing data size: 165 Performance of Testing

Model	F1 score	Sensitivity	Specificity	Epochs
Inception	90	48	100	20
Densenet-121	91	58	98	20

The values obtained for Inception model, Densenet121 model before and after gamma correction method displays the above table for 20 numbers of epochs

6.2.2 Without Gamma Correction for 10epochs

Training data size: 752 Testing data size: 188 Performance of Testing

Model	F1 score	Sensitivity	Specificity	Epochs
Inception	81	83	65	10
Densenet-121	80	77	72	10

With Gamma Correction (Gamma > 1)

Training data size: 703 Testing data size: 177 Performance of Testing

Model	F1 score	Sensitivity	Specificity	Epochs
Inception	71	71	49	10
Densenet-121	90	65	95	10

With Gamma Correction (Gamma < 1)

Training data size: 658 Testing data size: 165 Performance of Testing

Model	F1 score	Sensitivity	Specificity	Epochs
Inception	51	22	101	10
Densenet-121	79	42	101	10

The values obtained for Inception model, Densenet121 model before and after gamma correction method displays the above table for 10 numbers of epochs

6.3 GRAPH

The graph Figure 23 displays the x-axis shows the Gamma values and y-axis describes the percentage obtained of each model. The Gamma < 1 values shows the F1 score 91% which shows in blue color, Sensitivity rate is 58% which is shown in red color and Specificity rate as 98% again which is shown in green color. The Gamma $= 1$ values shows the F1 score 80% which shows in blue color, Sensitivity rate is 77%which is shown in red color and Specificity rate as 72% again which is shown in green color. The Gamma > 1 values shows the F1 score 83% which shows in blue colour, Sensitivity rate is 53% which is shown in red color and Specificity rate as 100% again which is shown in greencolor

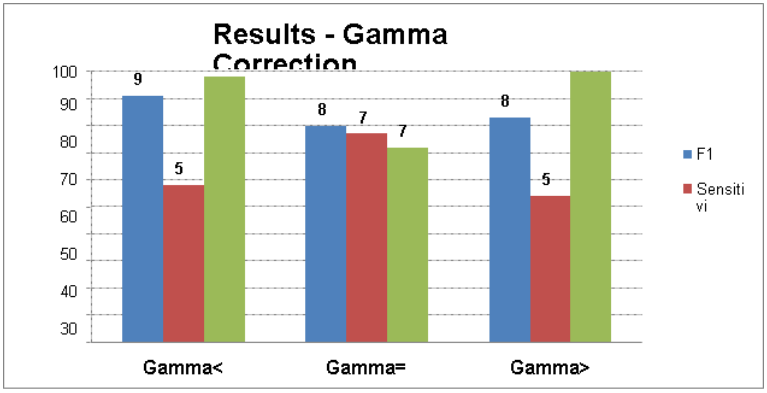

Figure 6.7: Results of Gamma Correction

In this section we have discussed about ROC Curve model, Comparison Table, Graph in next section we conclude the project and add reference.

Chapter 7

CONCLUSION

Prediction of cancerous or non-cancerous of chest X-rays was done where we have implemented on two models one is InceptionV3 model and on Densenet121 model and calculated Specificity, Sensitivity and F1 score for both models and we have achieved 0.95, 0.72, 0.82 over 20 respectively epochs on inceptionV3 model, and similarly on Densenet121model we have achieved 0.95, 0.72, 0.82 over 20 epochs respectively on InceptionV3 model 0.92, 0.79 0.85 respectively over 20 epochs. Then we have applied Gamma correction method where firstly we have tested for the gamma value < 1 over both the models and then we have tested for gamma value $>$ 0 for both the models. Through this experiment the gamma > 1 that is 1.5 gave us better results for both the models and we have predicted either the Chest x-ray is cancerous or normal. This experiment will complement the medical experts in taking diagnosticdecisions.

REFERENCES

[1] Syed Aley Fathima Syed Saba Raoof, M A Jabbar. Lung cancer prediction using machine learning: A comprehensive approach. *Lung Cancer*, 154, 01 2021.

[2] https://www.who.int/data/gho/data/themes/mortality-and-global-health estimates.

[3] Prajoy Podder Mondal 1 Subrato Bharati 1. Hybrid deep learning for detecting lung diseases from x-ray images. *Lung Cancer*, 154, 01 2021.

[4] M Rubaiyat Hossain Mondal 1 Subrato Bharati 1, Prajoy Podder 1. Weakly supervised learning for classification of lung cytological images using attention-based multiple instance learning. *Lung Cancer*, 154, 01 2021.

[5] https://www.cancerresearchuk.org/about-cancer/lung-cancer/stages-%20types-grades/stages grades.

[6] https://www.mariekeating.ie/cancer-information/lung-cancer/stages-types grades/:.

[7] Timor Kadir and Fergus Gleeson. Lung cancer prediction using machine learning and advanced imaging techniques. *Translational Lung Cancer Research*, 7(3), 2018.

[8] Timor Kadir and Fergus Gleeson. Lung cancer prediction using machine learning and advanced imaging techniques. *Translational Lung Cancer Research*, 7(3), 2018.

[9] Marjolein Heuvelmans, Peter Van Ooijen, and month = 01 pages = title = Lung cancer prediction by Deep Learning to identify benign lung nodules volume = 154 journal = Lung Cancer doi = 10.1016/j.lungcan.2021.01.027 , year = 2021.

[10] Pancreatic Cancer Survival Prediction: A Survey of the State-of-the Art. Pancreatic cancer survival prediction: A survey of the state-of-the-art. *Lung Cancer*, 154, 01 2021.

[11] A promising step forward for predicting lung cancer ShravyaShetty. M.s.i et.al. may 20 2019 lung cancer prediction using machine learning syed saba raoof. *Lung Cancer*, 154, 01 2021.

[12] Secil Genc, Kubra Nur Akpinar, and Serap Karagol. Automated abnormality classification of chest radiographs using mobilenetv2. In *2020 International Congress on Human-Computer Interaction, Optimization and Robotic Applications (HORA)*, pages 1–4, 2020.

[13] Md. Jahin Alam, Shams Nafisa Ali, and Md. Zubair Hasan. A robust cnn framework with dual feedback feature accumulation for detecting pneumonia opacity from chest x-ray images. In *2020 11th International Conference on Electrical and Computer Engineering (ICECE)*, pages 77–80, 2020.

[14] Secil Genc, Kubra Nur Akpinar, and Serap Karagol. [14] a promising step forward for predicting lung cancer shravyashetty, m.s.i. In *[14] A promising step forward for predicting lung cancer ShravyaShetty, M.S.i (HORA)*, pages 1–4, 2020.

[15] Kubra Nur and Serap Karagol. [15] a promising step forward for predicting lung cancer shravyashetty, m.s.i. In *[14] A promising step forward for predicting lung cancer ShravyaShetty, M.S.i (HORA)*, pages 1–4, 2020.